



Contents lists available at ScienceDirect

Spectrochimica Acta Part A: Molecular and Biomolecular Spectroscopy

journal homepage: www.elsevier.com/locate/saa

Synthesis and electrochromic, acidochromic properties of Schiff bases containing triphenylamine and thiophene units



Xiaotong Wu^a, Wen Wang^{b,*}, Bin Li^a, Yanjun Hou^a, Haijun Niu^{a,*}, Yanhong Zhang^a, Shuhong Wang^a, Xuduo Bai^a

^a Key Laboratory of Functional Inorganic Material Chemistry, Ministry of Education, Department of Macromolecular Science and Engineering, School of Chemistry and Chemical Engineering, Heilongjiang University, Harbin 150086, PR China

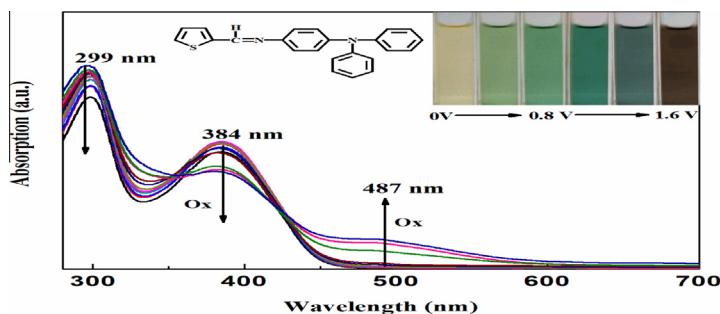
^b School of Material Science and Engineering, Harbin Institute of Technology, Harbin 150080, PR China

HIGHLIGHTS

- The SBs have excellent solubility in common organic solvents.
- The SBs exhibit stable electrochromic with stability.
- The SBs show acidochromic properties with good reversibility.
- The SBs are sensitive to pH values.

GRAPHICAL ABSTRACT

Electronic absorption spectra of SB1 with being doped electrochemically.



ARTICLE INFO

Article history:

Received 11 October 2014

Received in revised form 18 December 2014

Accepted 5 January 2015

Available online 13 January 2015

Keywords:

Triphenylamine
Electrochromic
Acidochromic
Schiff base
Electrochemical

ABSTRACT

A series of Schiff bases (SBs) were designed and prepared from 2-thiophenecarboxaldehyde and different triphenylamine (TPA) derivatives. The structures of the compounds were characterized by Fourier transform infrared (FT-IR), hydrogen nuclear magnetic resonance (¹H NMR). The optical and electrochemical properties were tested by ultraviolet–visible (UV–vis) spectroscopy and cyclic voltammetry (CV) techniques. The SBs exhibited stable and reversible electrochromic properties. Furthermore, multiple reversible colors states were also observed with the change of pH. Consequently, the SBs can be used as electrochromic and acidochromic materials.

© 2015 Elsevier B.V. All rights reserved.

Introduction

Electrochromic materials are a kind of functional materials which have broad applications in the flat panel display, information storage, glare-free mirror, smart window and other fields. Organic electrochromic materials have become the focus in the

field of electrochromism for many advantages, which including high color contrast ratios and multicolor capability. Near-infrared (NIR) absorption electrochromic materials are drawing more attention due to their potential applications in biological sensing, data storage, optical communication, thermal emission and thermal control detectors for spacecraft.

The SBs are synthesized by condensation of primary amines or amino compounds and carbonyl compounds. The structures of SBs are generally denoted as R₁R₂C=NR₃ (R₁ = H, R₂ or R₃ = alkyl, aryl

* Corresponding authors.

E-mail address: haijunniu@hotmail.com (H. Niu).

or heterocycle), which have the conjugated moiety, imine groups (C=N) in the backbone which are similar to —C=C— group with isoelectronic characteristics, planar configurations and optical behaviors [1]. SBs exhibit the ability of capturing proton, excellent thermal stability, good mechanical properties and metal-chelating ability. SBs would be the suitable alternative for electronic applications, pH and ion sensors [2], molecular wires [3], organic light-emitting diodes (OLED) [4], non-linear optical devices [5] and organic photovoltaics [6].

The TPA unit is easy to be oxidized in the nitrogen center and has the excellent ability to transport carriers via the radical cation species [7,8]. In the year of 2008, Iwan group investigated deeply on a series of aromatic polyazomethines with attractive optic-electronic properties bearing TPA [9]. TPA derivatives have showed excellent thermal and electrochemical stability, electron-donating ability and optoelectronic properties which have been used as advanced materials for memories, electroluminescence and photoelectric devices [10–14]. Thiophene derivatives have attracted great attention owing to the outstanding stability and optical properties. Silvia Destri et al. designed and studied a great amount of electrochromic materials made from thiophene derivatives [15]. Skene et al. also synthesized a series of azomethines containing thiophene with low optical band gaps (1.3–2.0 eV), and all polymers were claimed to be chemically and photochemically stable [16]. The introduction of thiophene increased the overall conjugation and improved the opto-electronic properties. SBs were suitable for electronic materials due to reversible acid doping, reoxidation and electrochromic properties. The variation of the backbone structure distinctly affected the dihedral angles and changed the electronic properties of SBs.

In this article, we reported a series of novel SBs compounds, which synthesized from thiophene aldehyde with five different amines containing TPA. The structures of the compounds were characterized by ^1H NMR and FT-IR. The optical, acidochromic properties were tested by UV-visible spectroscopy and electrochemical properties were tested by CV techniques. By being doped HCl vapor, the color of most SBs changed from yellow to red. The change trend of E_g measured experimentally is consistent with the theoretical value, which is calculated through quantum chemical simulation. The designed SBs provide indispensable materials for the electrochromic and acidochromic field.

Experimental

Materials

5% palladium on activated carbon (Pd-C) was purchased from Acros. 4-fluoronitrobenzene, N,N-dimethylformamide (DMF), dimethylsulfoxide (DMSO, A.R.) were supplied from Sinopharm Chemical Reagent, and used as received. DMF and DMSO were dried over CaH_2 and distilled under reduced pressure. Lithium perchlorate (LiClO_4) was dried under vacuum at 120°C for 36 h. 4-amino-triphenylamine (A1), 4,4'-diamino-triphenylamine (A2) and 4,4',4''-triamino-triphenylamine (A3) were synthesized by Pd/C-catalyzed reduction of the corresponding nitro-compounds obtained from the reaction of diphenylamine derivatives with 4-fluoronitrobenzene in the presence of sodium hydride. 4-methyl-4',4''-diamino-triphenylamine (A4), 4-ethoxy-4',4''-diamino-triphenylamine (A5) and thiophene formaldehyde were synthesized according to the references [17–22].

Measurements

The obtained compounds were characterized by the following techniques: FT-IR spectra were measured on a PerkinElmer Spec-

trum 100 Model FT-IR spectrometer. Using tetramethylsilane as an internal reference, ^1H NMR spectra were recorded on a Bruker AC-400 MHz spectrometer in CDCl_3 . UV-vis spectra were conducted on a UV-3600 (Shimadzu). The electrochemical and electrochromic properties of the SBs were determined by CV techniques and UV-vis spectroscopy. For the electrochromic investigations, a homemade electrochemical cell was built from a commercial UV-vis cuvette. The cell was placed in the optical path of the sample light beam in a UV-vis spectrophotometer to acquire electronic absorption spectra under potential control in a 0.1 M solution of LiClO_4 as an electrolyte under nitrogen atmosphere in dry CH_3CN . CV was conducted on a CH Instruments 660 A electrochemical analyzer at a scan rate of 50 mV/s in 0.1 M $\text{LiClO}_4/\text{CH}_3\text{CN}$ with the use of a three-electrode cell in which ITO-coated was used as a working electrode. The oxidation and reduction potentials of SBs were taken with the use of an Ag/AgCl reference electrode, a platinum wire being used as an auxiliary electrode, and were calibrated against the ferrocene/ferrocenium (Fc/Fc^+) redox couple. The pH values were determined by using the SARTORIUS PB-10 pH meter, which were calibrated by standard buffer solutions of pH 4.01 and 6.86. The pH value of solution was adjusted by addition of HCl vapor to 0.1 M DMSO/ H_2O solution.

Synthesis of monomer

4-methyl-4',4''-diamino-triphenylamine (A4), 4-ethoxy-4',4''-diamino-triphenylamine (A5), 2-thiophenecarboxaldehyde, have been synthesized, and corresponding spectra are presented in [Supporting Information](#).

A4: FT-IR: (KBr, v/cm^{-1}): 3407 (N–H stretching), 1592, 1509, 1490 (aromatic ring of benzene), 1314, 1280 (C–N stretching).

^1H NMR: (CDCl_3 , 400 M): 6.54, 6.87, 7.32 (aromatic ring of triphenylamine), 1.67 (CH_3), 4.26 (NH_2).

A5: FT-IR: (KBr, v/cm^{-1}): 3398 (N–H stretching), 1585, 1505, 1493 (aromatic ring of benzene), 1314, 1280 (C–N stretching).

^1H NMR: (CDCl_3 , 400 M): 6.54, 6.63, 7.03 (aromatic ring of triphenylamine), 4.07 (CH_2), 1.47 (CH_3), 4.26 (NH_2).

2-thiophenecarboxaldehyde: FT-IR: (KBr, v/cm^{-1}): 2753 (C–H stretching), 1708 (C=O stretching).

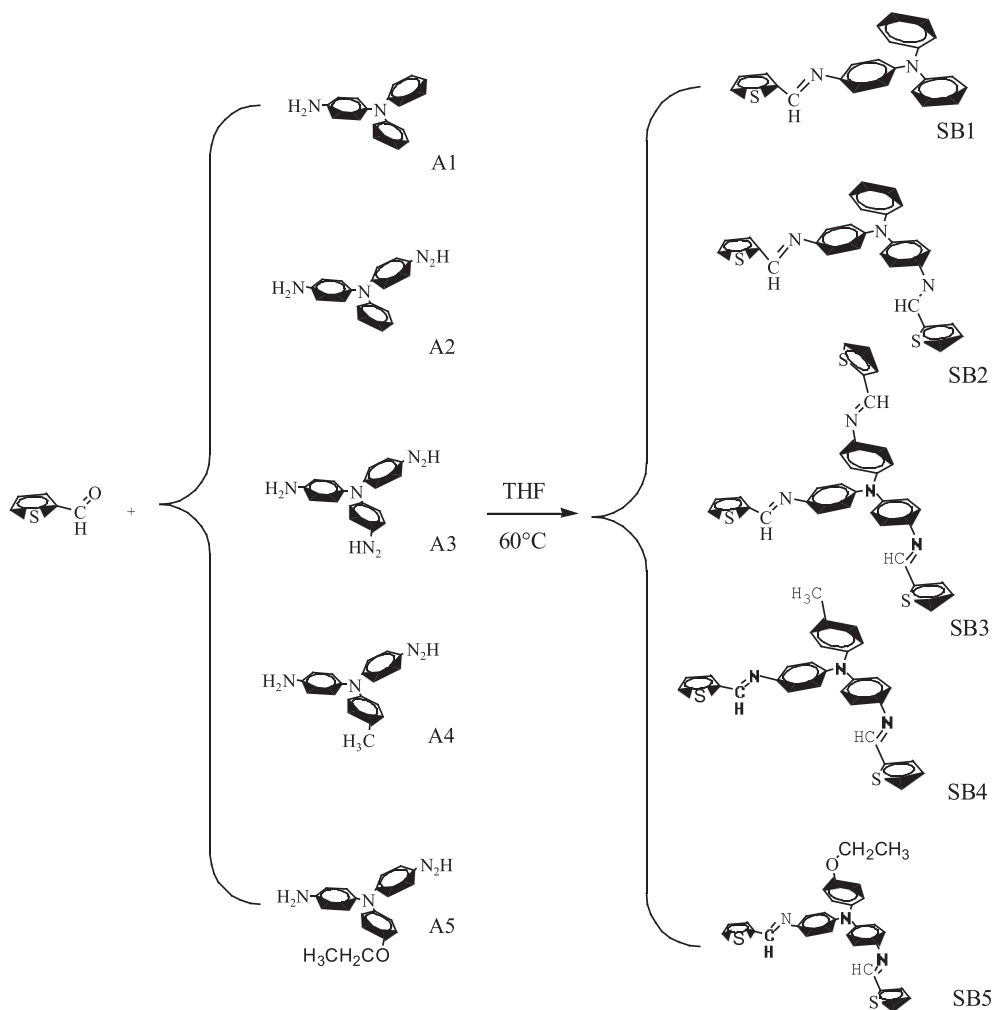
^1H NMR: (CDCl_3 , 400 M): 10.15 (CH=O), 7.39, 8.07, 8.22 (thiophene ring-H).

Synthesis and characterization of SBs

Take preparation of SB1 for example: 4-amino-triphenylamine (A1) (0.5217 g, 0.0020 mol) was dissolved in 100 ml THF and the mixture was poured into a 100 ml, three-neck, round-bottom flask. 2-thiophenecarboxaldehyde (0.3017 g, 0.0027 mol) was added slowly into the mixture, then a drop of acetic acid was added. After that the solution was stirred at 60°C reflux temperature for 4 h under nitrogen atmosphere, it became transparent and orange. The solution was evaporated by rotary evaporation to powders in brown with the yield of 73.1% (0.5174 g). The other SBs were prepared in the same procedure, and the synthesis routes of SBs are showed [Scheme 1](#).

SB1: ^1H NMR: (CDCl_3 , 400 M): 8.628 (s, 1), 7.47–7.56 (m, 1), 7.15–7.21 (m, 6), 7.10–7.14 (m, 2), 7.02–7.06 (d, 6); FT-IR: (KBr, v/cm^{-1}): 2925, 2869, 1613, 1597, 1581, 1480, 833, 719; yield 73.81% (0.5174 g), melt point (mp) $158\text{--}159^\circ\text{C}$.

SB2: ^1H NMR: (CDCl_3 , 400 M): 8.638 (s, 2), 7.46–7.52 (m, 2), 7.15–7.23 (d, 6), 7.03–7.10 (m, 1), 6.92–7.02 (d, 6), 6.65–6.70 (d, 4); FT-IR: (KBr, v/cm^{-1}): 3031, 2922, 2868, 1611, 1510, 1491, 826, 715; yield 66.3% (0.6759 g), melt point (mp) $174\text{--}175^\circ\text{C}$.



Scheme 1. The synthesis routes of SBs.

SB3: $^1\text{H NMR}$: (CDCl_3 , 400 M): 8.630 (s, 3), 7.41–7.53 (m, 3), 7.06–7.18 (d, 6), 6.91–7.03 (d, 6), 6.60–6.70 (d, 6); FT-IR: (KBr, v/cm^{-1}): 3030, 2928, 2865, 1608, 1507, 1492, 827, 715; yield 68.3% (0.5472 g), melt point (mp) 184–186 °C.

SB4: $^1\text{H NMR}$: (CDCl_3 , 400 M): 8.633 (s, 2), 7.49–7.55 (m, 2), 7.14–7.22 (d, 8), 7.10–7.13 (d, 2), 7.04–7.08 (d, 4), 6.96–7.02 (d, 2), 2.357 (s, 3); FT-IR: (KBr, v/cm^{-1}): 3029, 2917, 2864, 1608, 1494, 831, 708; yield 59.9% (0.6007 g), melt point (mp) 156–158 °C.

SB5: $^1\text{H NMR}$: (CDCl_3 , 400 M): 8.630 (s, 2), 7.47–7.51 (d, 2), 7.04–7.19 (d, 8), 6.82–6.98 (d, 6), 6.62–6.69 (d, 2), 3.98–4.11 (q, 2), 1.39–1.49 (t, 3); FT-IR: (KBr, v/cm^{-1}): 3034, 2974, 2926, 2867, 1610, 1497, 1475, 1237, 825, 711; yield 64.4% (0.5882 g), melt point (mp) 132–133 °C.

Results and discussion

$^1\text{H NMR}$ analysis

As for the $^1\text{H NMR}$ data, take SB5 for example: as shown in Fig. 1, the chemical shift at 8.63 is attributed to H in $-\text{CH}=\text{N}-$, which shows that the target SB5 is obtained successfully. Chemical shifts at 7.47–7.51 are attributed to H in thiophene ring. Chemical shifts at 7.04–7.19, 6.82–6.98, 6.62–6.69, 3.98–4.11 and 1.39–1.49 are attributed to hydrogen in thiophene ring and in benzene ring.

As shown in Fig. S1, the main peaks are at about 8.70, where the chemical shifts are ascribed to the proton at the $\text{H}-\text{C}=\text{N}-$. Between the 9.0 and 10.0, no peaks are discovered, which indicating that 2-thiophenecarboxaldehyde has been reacted completely.

FT-IR analysis

The FT-IR spectra of the SBs are shown in Fig. 2(a). The distinct absorption peak at 1610 cm^{-1} confirms the existence of $-\text{C}=\text{N}-$ group. There is not absorption peak of $\text{N}-\text{H}$ around 3034 cm^{-1} and 2974 cm^{-1} , which proves the reaction is completed. The characteristic peaks of aromatic group of SB1–SB5 are observed at 2924 cm^{-1} and 2854 cm^{-1} , corresponding to $-\text{C}-\text{H}-$ stretching vibrations of thiophene and benzene groups, respectively. There are peaks at 1497 and 1475 cm^{-1} owing to $-\text{C}=\text{C}-$ groups, 1237 cm^{-1} owing to the $\text{C}-\text{S}-\text{C}$ stretching vibration of thiophene. The bands at around 825, 711 cm^{-1} are due to $\text{C}-\text{S}-\text{C}$ stretching vibration in $-\text{OCH}_2\text{CH}_3$.

In order to illustrate the $-\text{C}=\text{N}-$ band change of SBs in organic solvents, we also measured the FT-IR spectra of SB4 and SB5 in tetrahydrofuran (THF) about protonation/deprotonation. Fig. 2(b) shows the FT-IR spectra of SB5 before and after the solution was exposed to HCl and NH_3 vapor. $-\text{C}=\text{N}-$ main vibration bands are observed at 1616 cm^{-1} before the solution was exposed to HCl. After being exposed to HCl vapor, the stretching vibration of $-\text{C}=\text{N}-$ moiety at 1616 cm^{-1} disappeared, while peak at

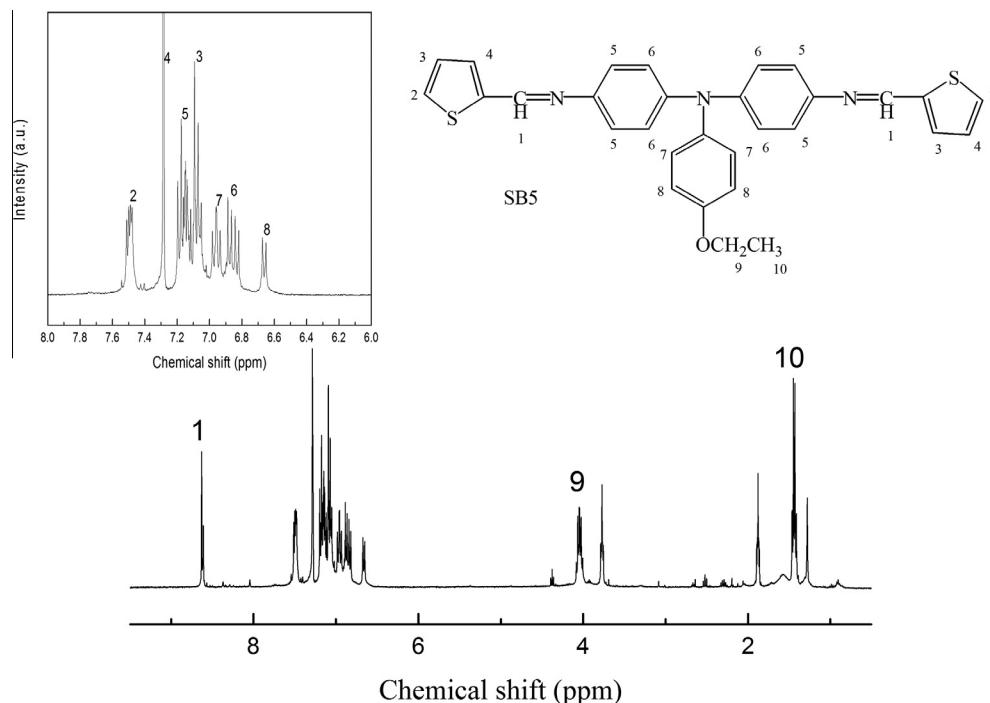


Fig. 1. ^1H NMR spectra of SB5.

1627 cm^{-1} appeared due to the stretching vibration of $\text{C}=\text{NH}^+$ [23]. After being exposed to NH_3 vapor, the absorption peak at 1627 cm^{-1} went back to the original 1618 cm^{-1} , but the peak strength became weak due to the production of NH_4Cl . The similar FT-IR spectra of SB4 in THF about protonation/deprotonation is shown in Fig. S2.

UV–vis absorption spectra analysis

The UV–visible absorption spectra of SBs measured in DMSO solutions are shown in Fig. 3. All the UV absorption peaks of SBs exhibit strong absorption at 380–410 nm, which are assigned to a $\rho\text{-}\pi$ transition resulted from the conjugated TPA segment and $\text{C}=\text{N}$ double bonds in the backbone. Different spectra of SBs perhaps owe to the different substituted structures which have different electronic cloud in the repeat unit. The λ_{max} s are arranged in the order: $\text{SB3} > \text{SB5} > \text{SB4} > \text{SB2} > \text{SB1}$. Comparing the structure of SB1, SB2 and SB3, three H atoms at the end of the TPA in SB3 are replaced by three 2-aldehyde thiophene. The obtained product has three arms with highly conjugated state of electron cloud so that the lowest-unoccupied molecular orbital (LUMO) was reflected by the larger maximum absorption wavelength. As for SB2 with two arms, the whole electron cloud is less than that of SB3 and the maximum absorption wavelength is shorter than SB3. SB1 with only one 2-aldehyde thiophene group has the lowest conjugated state relatively. Compared with SB2 and SB3, the whole electron cloud of SB1 is less than the others, and the maximum absorption wavelength is blue shifted. Take SB2, SB4, and SB5 for comparison, they have similar two conjugated arms. However, the third arm was replaced by hydrogen, methyl and oxethyl groups, respectively. Oxethyl group made the electron clouds of the whole molecule easier to flow than that of methyl group and hydrogen. So among SB2, SB4 and SB5, λ_{max} of SB5 was red shifted most, while λ_{max} of SB2 was red shifted least.

Electrochemical properties

The electrochemical behaviors of the SBs were investigated by CV techniques. The electrochemical spectra of SB1–SB5 are shown in Fig. 4. All the SBs (SB1–SB5) exhibit one pair of obvious reversible redox peaks which are corresponding to the oxidation of the TPA moiety [24]. It can be understood that the conjugated degree, the pulling and pushing electron properties of different groups would influence the redox potentials. SB3 has the lowest electronic energy level (compared to SB1, SB2 and SB3) due to three arms structure having the higher conjugated state and needing more energy to be oxidized. SB5 with oxethyl group has the lowest energy level (compared to SB1, SB4 and SB5), which is attributed to the pushing electron nature of ethoxyl group which makes electron cloud move to benzene ring of TPA.

To further understand the electronic structures of the SBs, and to provide key parameters for the design of devices, it is necessary to determine the highest occupied molecular orbital (HOMO) and LUMO energy levels of the SBs. The Fc/Fc^+ couple was used to calculate the onset oxidation potentials (E_{onset}) or half-wave potentials ($E_{1/2}$) whose redox potential is assumed to have an absolute energy level of -4.80 eV in vacuum to obtain accurate redox potentials of electrode. Thus, the HOMO energy values were calculated using the equation as follows [25,26].

$$E_{\text{HOMO}} = -e(E_{\text{onset vs Ag/AgCl}}^{\text{OX}} + 4.36)\text{ eV}$$

where $E_{\text{onset}}^{\text{OX}}$ is the onset oxidation potential vs Ag/AgCl. The HOMO energy values of SB1–SB5 were calculated to be in the range from -4.67 to -5.13 eV . E_{HOMO} of SBs could be determined from the onset oxidation potentials and the onset absorption wavelength which are listed in Table 1. The LUMO energy levels of the SBs were estimated from the HOMO energy levels because of the reduction curves could be hardly obtained by using the following equation:

$$E_{\text{LUMO}} = E_{\text{HOMO}} + E_{\text{g}}$$

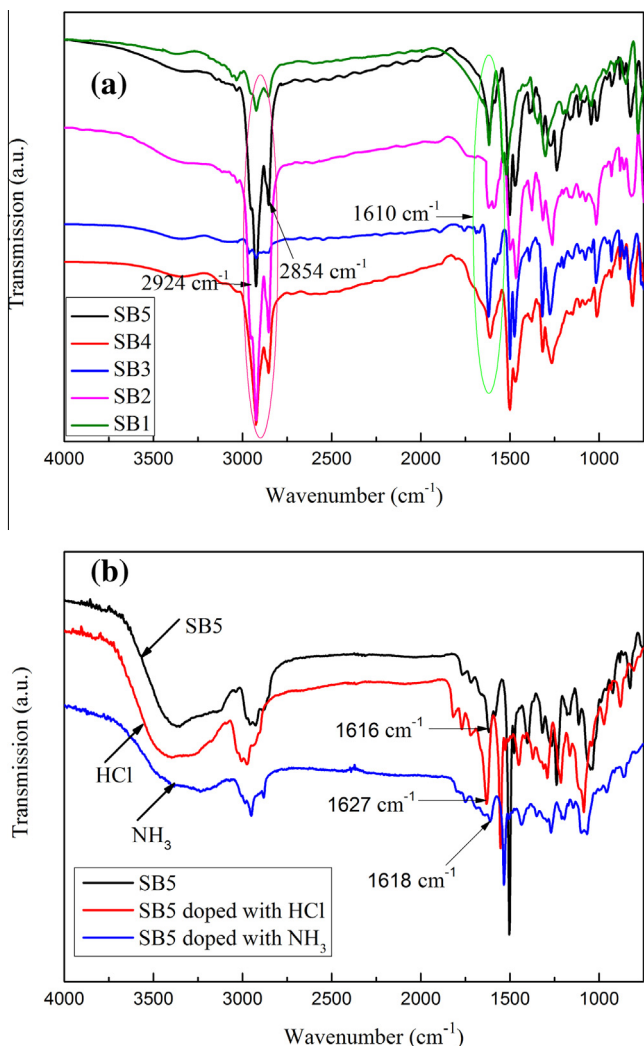


Fig. 2. FT-IR spectra of SBs. (a) SB1 to SB5; (b) SB5 before and after the solution was exposed to HCl and NH₃ vapor in THF.

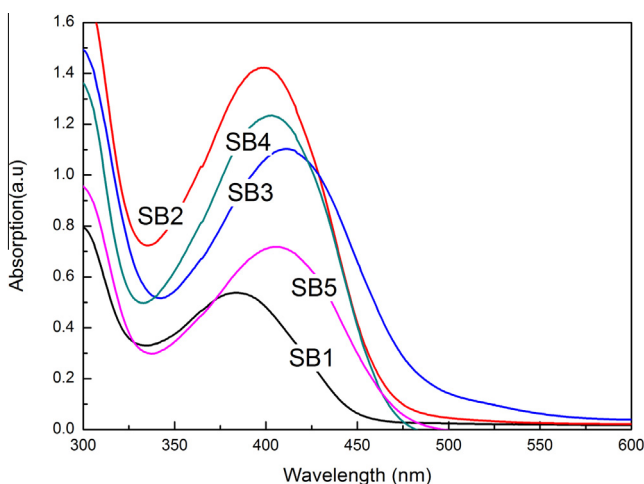


Fig. 3. The UV-vis spectra of SB1 to SB5.

And the optical band gap (E_g) was determined as follows:

$$E_g = 1240/\lambda_{\text{onset}}$$

The energy levels and optical band gaps have been presented in Table 1. Of the SBs, SB5 shows the highest HOMO, on the contrary,

the SB1 exhibits the lowest HOMO. SB5 shows the lowest E_g (2.56 eV), and the SB1 exhibits the highest E_g (2.75 eV).

Quantum chemical calculation

The ground-state geometries of the compounds were optimized by hybrid density functional theory (B3LYP) with 6-31 G basis set in the Gaussian 98 program package, and are presented in Fig. 5. For these SBs, the electronic wave-function of the HOMO is distributed entirely over the TPA moiety, which is beneficial for obtaining higher hole mobility. However, the electron wave-function of LUMO is mainly localized on the whole molecule. The whole molecular segment effectively reduced the band gap due to the low LUMO energy level of the SBs unit. The lone pair of electrons on the nitrogen atoms had strong coupling with π -electrons in TPA which led to an intramolecular charge transfer (ICT) with significant distribution of the electronic density over the entire molecule. As can be seen in Fig. 5, the HOMO energy level of SBs are in the order of SB5 > SB4 > SB2 > SB3 > SB1. It indicated that SB1 has the strongest antioxidation property among the studied polymers due to the lowest experimental HOMO energy level. The theory trend of E_g for the SBs series follows in the order: SB5 < SB3 < SB4 < SB2 < SB1 which basically corresponds with the experimental data in the order: SB5 < SB3 < SB4 < SB2 < SB1 (Table 1). The different groups linked TPA played the key role in the electron structure and regulated the gaps of SBs. The suitable energy levels of the conjugated SBs indicated their potential applications in OLED or solar cell.

Electrochromic properties

The electrochromic behaviors of the SBs were investigated by using an optically transparent thin-layer electrode coupled with UV-vis spectrometry at different applied potentials. The electrode and solution were identical to those used in CV. All SBs exhibit similar electrochromic properties, and the typical electrochromic absorption spectra of SB1 is shown in Fig. 6. In the neutral form, the SB1 exhibits strong absorption at wavelength around 299 nm and 384 nm. As the applied potential is raised, the SB1 shows a decreasing absorption at 384 nm with a concomitant appearance peak at 487 nm. The color of SB1 changes from original yellow to green, then to brown. SB2, SB3, SB4 and SB5 exhibit similar electrochromic properties, with the color of solution changing from original yellow to brown, then to red. N atom of TPA doped by oxidation results in the planar backbone, which leads to an increased π -electron delocalization. These changes may also originate from the enhanced charge transfer (CT) due to the stronger electron-donating moiety of TPA and the stronger electron-accepting center (that is N⁺) by doping the C=N in SBs. Similar electrochromic behaviours of other SBs are observed in Fig. S3.

Redox process and the resonance form of SBs

In order to neutralize the charge, the molecule would possess positive charge and anions of electrolyte would insert into the molecule matrix when SBs are at oxidative states. Scheme 2 shows the simplified redox process and the resonance form of SBs, in which N atom is the redox reaction centers corresponding to the various stages of electrochemical reactions. The electronic resonance of TPA groups would be affected by the substituent group, $-\text{HN}=\text{C}-$, which is electron withdrawing group and will further influence the electronic configurations of entire molecule. SBs are oxidized to their radical cation state when the applied voltage increased, then a successive resonant reactions would occur.

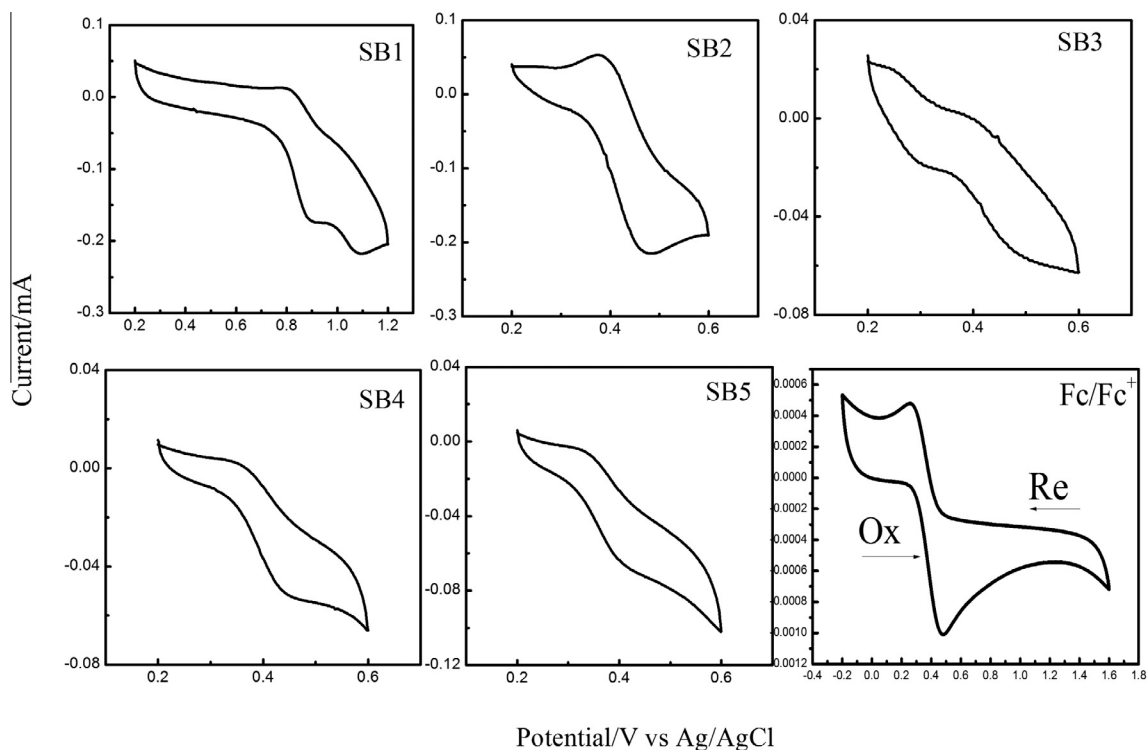


Fig. 4. CVs for SBs in 0.1 M LiClO₄/CH₃CN with Fc/Fc⁺ as an internal standard at the scanning rate of 50 mV/s.

Table 1
Electrochemical properties and energy levels of SB1 to SB5.

	λ_{onset} nm	$E_{\text{onset}}^{\text{OX}}$ eV	E_{HOMO} eV	E_{LUMO} eV	E_{g} eV	$E_{\text{HOMO}}^{\text{quantum}}$ eV	$E_{\text{LUMO}}^{\text{quantum}}$ eV	$E_{\text{g}}^{\text{quantum}}$ eV
SB1	450	0.78	-5.13	-2.38	2.75	-4.87	-1.68	3.18
SB2	467	0.37	-4.72	-2.06	2.65	-4.79	-1.77	3.01
SB3	480	0.37	-4.72	-2.14	2.58	-4.76	-1.82	2.94
SB4	469	0.34	-4.69	-2.05	2.64	-4.72	-1.75	2.96
SB5	483	0.32	-4.67	-2.10	2.56	-4.66	-1.74	2.92

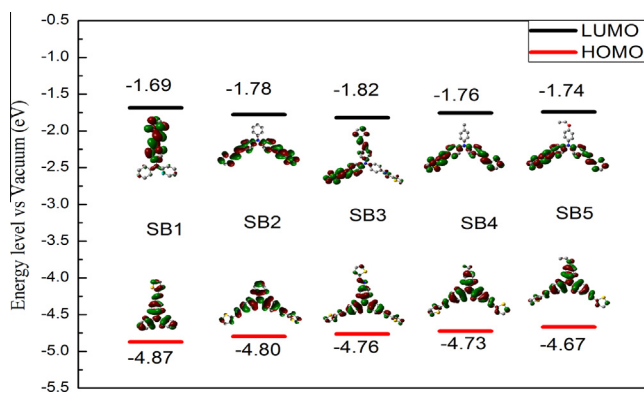


Fig. 5. Pictorial representations of the electron density in the frontier molecular orbitals of SBs.

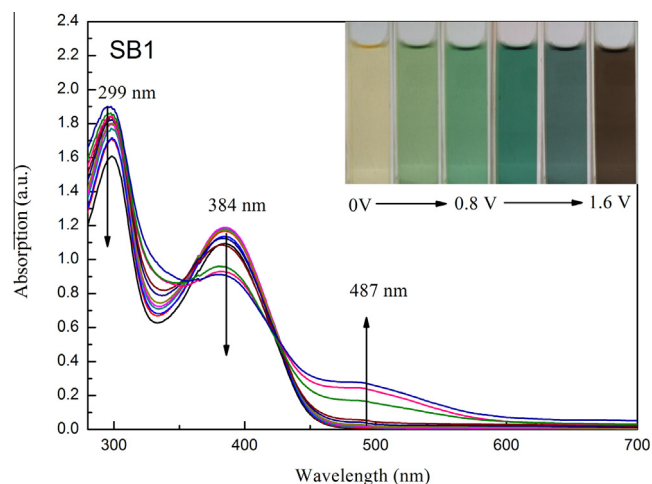
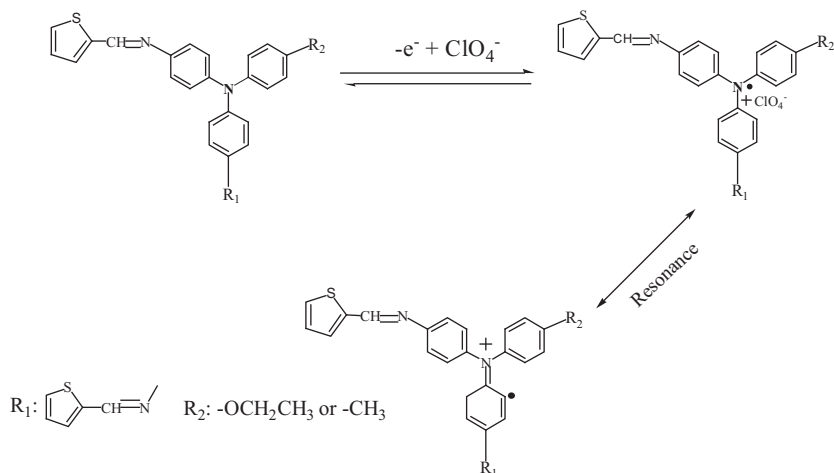


Fig. 6. Electronic absorption spectra of SB1 doped electrochemically.

Spectroelectrochemical properties

Optical switching were investigated to manifest the outstanding electrochromic characteristics of these obtained novel electro-

chromic materials. The electrode and solution are identical to those used in CV. Optical switching studies of SB3 are shown in Fig. 7 (the others are listed in Fig. S4 in Supporting Information). The color switching times are estimated by applying a potential step, and



Scheme 2. The simplified redox process of SBs from their neutral state to radical cation state.

the absorbance profiles are followed. The switching time is defined as the time required for reach 90% of the full change in absorbance after the switching of the potential. At 0.78 V, the SB3 requires 4.2 s for switching absorbance and 2.4 s for bleaching at 487 nm. When the potential is set at 1.0 V, the SB3 requires 3.8 s for coloration and 3.2 s for bleaching at 530 nm. After continuous cyclic scans between 0.00 V and 1.0 V in 300 s, the SBs still exhibit stable electrochromic characteristics, with the color switching time being slower than the bleaching switching time of 0.6 s. The electrochromic coloration efficiency (CE; η) is also an important characteristic for the electrochromic materials. CE can be calculated using the equations given below [27]:

$$\delta_{OD} = \lg(T_b/T_c)$$

$$\eta = \delta_{OD}/Q$$

where T_b and T_c are the transmittances before and after coloration, respectively; δ_{OD} is the change of the optical density, which is proportional to the amount of created color centers; η denotes the CE and Q (mC/cm^2) is the amount of injected/ejected charge per unit sample area. Through the table, we could conclude that CE is in the order: SB3 > SB5 > SB4 > SB2 > SB1. The SB3 exhibited highly stable electrochromic properties with the high CE up to $53.5 \text{ cm}^2/\text{C}$ at 530 nm (the others are listed in Table S1 in Supporting Informa-

tion), due to the planarity between bond of C=N and benzene ring which were linked together.

Acidochromic properties and pH sensor

The acidochromic characteristic of SB1 is shown in Fig. 8. Initially, neutral SB1 reveals the absorption maxima at 299 nm and 384 nm in DMSO solution, respectively. Neutral solution of SB1 is colorless. The proton concentrations were modulated by adding HCl vapor. After a neutral DMSO/H₂O solution of SB1 was exposed in HCl vapor, the absorption was substantially changed and the color of solution turned into red. HCl vapor being added every ten seconds, the intensity of the absorption peak at 299 and 384 nm gradually decreased while two new absorption bands at 487 and 323 nm gradually increased with pH value decreasing, which meant the absorption maxima of the SB1 was red-shifted. The corresponding pH values of SBs are determined by pH meter which are labeled in Fig. 8. The pH values of SB1 are ranging from 10.72 of initially neutral state (curve a) to 3.76 (curve j). N atom of the imine linkage being doped by acid results in the planar backbone and an increased π -electron delocalization. On the other

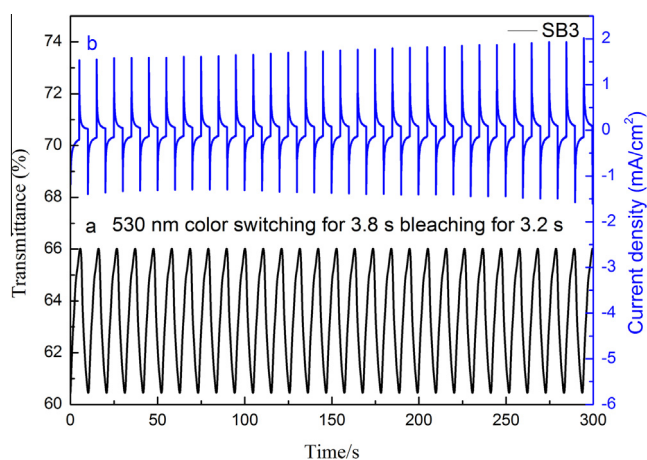


Fig. 7. Optical switching procedures: (a) potential step absorptometry of SB3 at 530 nm (0.1 M LiClO₄ as the supporting electrolyte) by applying a potential step (0.0–1.0 V). (b) Current consumption of SB3.

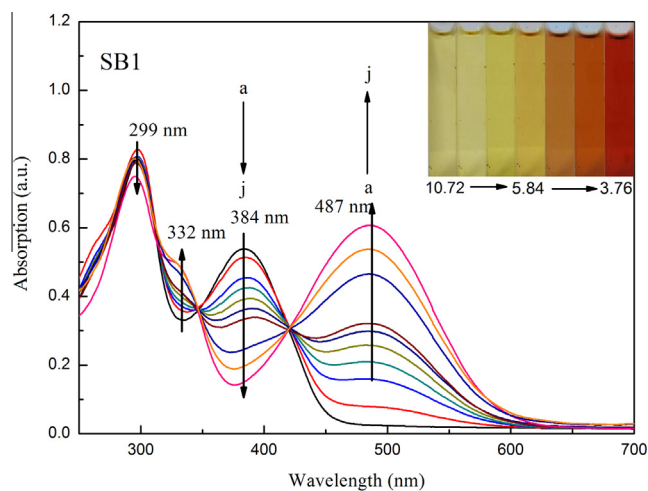


Fig. 8. The UV-vis absorption spectra of solution of SB1 protonated by HCl vapor in DMSO/H₂O (1:1, v/v) and in the same time interval. The concentration of SBs is $1.0 \times 10^{-5} \text{ M}$. Inset photographs indicate the color evolved in the process of being doped HCl vapor. The values of pH from a to j are: 10.72, 9.24, 7.12, 6.46, 5.84, 5.19, 4.76, 4.66, 4.14 and 3.76.

hand, as shown in the Scheme 3, the protonation and deprotonation of the $-\text{C}=\text{N}-$ ($-\text{C}=\text{N}^+-$) results in a stronger electron-accepting center, so that charge separation of π -electrons is enhanced in the conjugated SBs with donor-acceptor structure. Absorption spectra of SB1 reveal the existence of isoelectric point in solution, which confirms the coexistence of discrete chromophores. It is indicated that the solution possesses well reversible acidochromism. (Similar acidochromic characteristics of other SBs are observed in Fig. S5 in Supporting Information). The stability and responding time of the acidochromism of the SBs were measured by UV-visible spectroscopy and responding curve of SB1 is shown in Fig. 9. The responding time is measured to be 4 s and the bleaching time is 5.0 s which means the response is fast. After continuous several cyclic between HCl and NH_3 vapor, the transmittance decreased because of the production of NH_4Cl in the responding process. The SB3 (showed in Fig. S6) has the similar changes to SB1, but the switching time is different. Compared to the SBs, SB3 has a shorter color changing time (3.2 s) due to higher carrier mobility than other SBs.

We further studied the effect by varying the pH values of SBs on the absorption spectral properties in mixed solvent of DMSO/ H_2O . We chose six pH points to discuss in detail. The solution pH value ranged from 5.84 (curve e) to 3.76 (curve j). The intensity increased slightly after the pH was lowered further and reached some extent. A similar behaviour has also been observed for SB2, SB3, SB4 and SB5. It is interesting to study and compare the inorganic acid effect on the UV-vis absorption of SBs. It is observed that SBs are quite sensitive to pH value of solution. These investigations of optical property reveal that the sensors based on SB materials may be applied in convenient detecting apparatus for detection environmental proton. Moreover, the relationship between absorbance spectrum of the SB1 and pH is shown in Fig. 10(a). Relative absorbance intensities ($I - I_0/I_0$) at 384 nm are plotted vs. pH and a linear response for pH at 384 nm is obtained with a very good regression coefficient as $R = 0.9696$ (Fig. 10(a)). This linear response could be used for detection of pH range from 5.84 to 3.76 using the following equation:

$$(I - I_0/I_0) = 0.041 [\text{pH}] + 0.085 \quad (1)$$

where I is the absorbance intensity at different pH and I_0 is the absorbance intensity of pH is 5.84 at 384 nm. It is found that the absorbance decreases linearly with pH ranging from 5.84 to 3.76 at 384 nm. We attribute the reason to the level of protonation close to saturation with the H^+ concentration increasing. The other four SBs also have the similar behaviour of absorbance dependent on

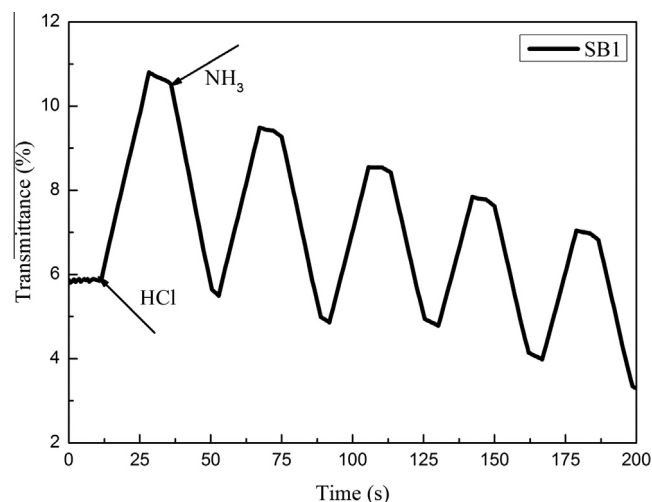
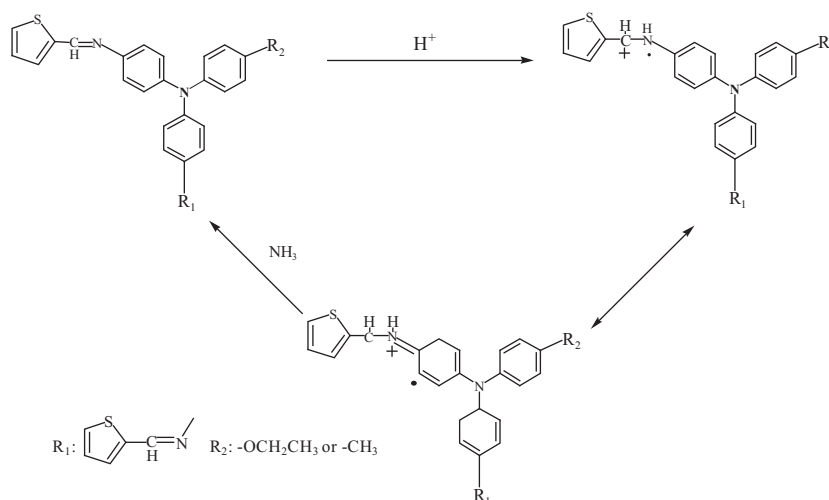


Fig. 9. UV-visible absorption spectra change of SB1 at 425 nm when repeatedly placed in HCl and NH_3 vapor.

pH value. As the HCl concentration had a proportionality with pH in our experiment, it indicated that the absorbance follows a linear relationship with HCl concentration. From Fig. 8, we can calculate the pK_a of SB1 according to Eq. (2) [28–30]:

$$A = A_A^- + [(A_{\text{HA}} - A)[\text{H}^+]/K_a] \quad (2)$$

Curve is plotted (Fig. 10(b)), where A is the solution absorbance of different pH, A_A^- and A_{HA} the absorbance of conjugated base and conjugated acid in their maximal concentrations at 332 nm. From the slope, we can get the $\text{pK}_a = 4.83$. The pK_a of protonated SB2, SB3, SB4, SB5 in solution (DMSO/water, 1: 1) was similar to that of the SB1 (4.83). From Fig. S5, we can calculate the pK_a of SB2, SB3, SB4, SB5 to be 5.24, 5.72, 5.38 and 5.63, respectively according to Eq. (2). The SB3 exhibits the highest pK_a (5.72) at 332 nm which can be explained by that SB3 has three imines providing most doping site. The SB1 shows the lowest pK_a (4.83) is probably due to that its electron-donating ability is weakest. SB5 is the second one because its ethoxy group has more inductive effect. The study of the pH effect on absorption spectra provides a good tool for researching interactions including hydrogen transfer processes between the color and its chemical condition.



Scheme 3. The protonation and deprotonation of the $\text{C}=\text{N}$ in SBs in HCl vapor and NH_3 vapor.

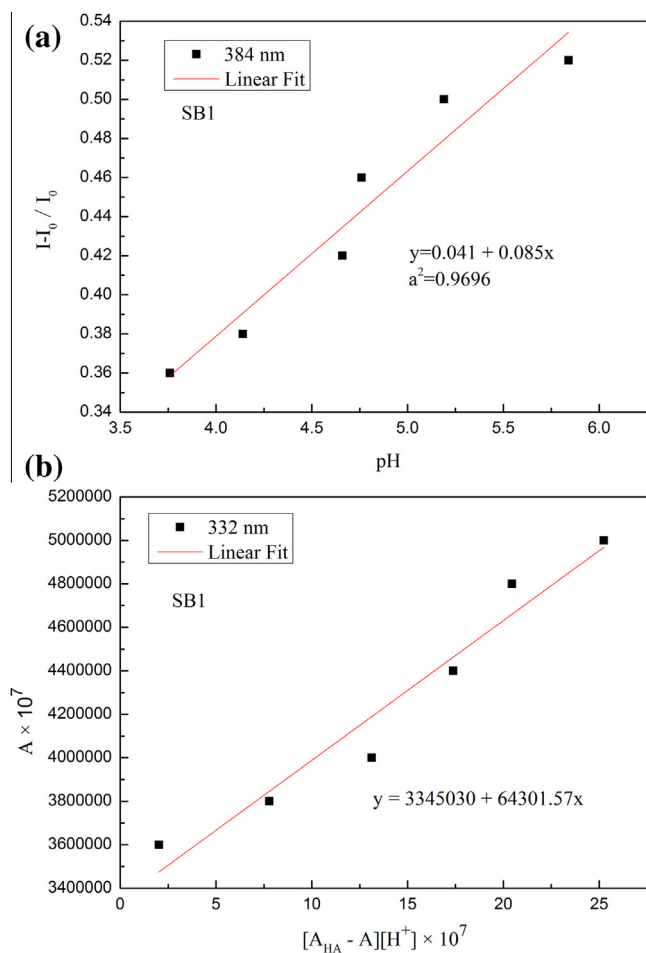


Fig. 10. (a) The change of absorbance with pH ranging from 5.84 to 3.76 at 384 nm. (b) $A - (A_{\text{HA}} - A) [\text{H}^+]$ plot of different pH at 332 nm.

Conclusions

A series of highly stable anodic electrochromic SBs with excellent optical transmittance change have been synthesized from 2-thiophenecarboxaldehyde and different TPAs. The SBs exhibit excellent reversible electrochemical behavior and continuous cyclic stability of electrochromic characteristics and electrochromic reversibility. SBs are also sensitive to the pH values, especially. The calculated HOMO and LUMO energy levels of the SBs by experimental method are identical to theoretical calculation, respectively. The SBs not only provide new products for the electrochromic material, but also provide theoretical basis for the electrochromic process of polymers.

Acknowledgements

The authors were grateful to the support of the National Science Foundation of China (Grant Nos. 51373049, 51372055, 51273056, 21372067, 21206034), Doctoral Fund of Ministry of Education of China (20132301120004, 20132301110001).

Appendix A. Supplementary data

Supplementary data associated with this article can be found, in the online version, at <http://dx.doi.org/10.1016/j.saa.2015.01.007>.

References

- [1] S. Dufresne, A. Bolduc, W.G. Skene, *J. Mater. Chem.* 20 (2010) 4861–4866.
- [2] M.A. Neelakantan, M. Esakkiammal, S.S. Mariappan, J. Dharmaraja, T. Jeyakumar, *Indian J. Pharm. Sci.* 72 (2010) 216–222.
- [3] M.J. Frampton, H.L. Anderson, *Angew. Chem. Int. Ed.* 46 (2007) 1028–1064.
- [4] Y. Fan, H.M. Zhang, J.S. Chen, D.G. Ma, *Org. Electron.* 14 (2013) 1898–1902.
- [5] Q.M. Liu, X.J. Zhao, *J. Non Cryst. Solids* 356 (2010) 2375–2377.
- [6] Y.C. Chen, C.Y. Yu, Y.L. Fan, L.I. Hung, C.P. Chen, C. Ting, *Chem. Commun.* 46 (2010) 6503–6505.
- [7] É. Knipping, I.U. Roche, S. Dufresne, N. McGregor, W.G. Skene, *Tetrahedron Lett.* 52 (2011) 4385–4387.
- [8] A. Iwan, D. Sek, *Prog. Polym. Sci.* 36 (2011) 1277–1325.
- [9] D. Sek, A. Iwan, B. Jarzabek, B. Kaczmarczyk, J. Kasperczyk, Z. Mazurak, M. Domanski, K. Karon, M. Lapkowski, *Macromolecules* 41 (2008) 6653–6663.
- [10] H.Y. Jin, X.G. Li, T.F. Tan, S.R. Wang, *Dyes Pigm.* 106 (2014) 154–160.
- [11] L.Z. Liu, X.F. Meng, W. Li, X.Q. Zhou, Z.C. Bai, D.Z. Liu, Y.R. Lv, R.H. Li, *Dyes Pigm.* 108 (2014) 32–40.
- [12] H.M. Wang, S.H. Hsiao, *J. Polym. Sci. A Polym. Chem.* 52 (2014) 1172–1184.
- [13] M. Grigoras, T. Ivan, L. Vacareanu, A.M. Catargiu, R. Tigoianu, *J. Lumin.* 153 (2014) 5–11.
- [14] S. Suzuki, Y. Matsumoto, M. Tsubamoto, R. Sugimura, M. Kozaki, K. Kimoto, M. Iwamura, K. Nozaki, N. Senju, C. Uragami, H. Hashimoto, Y. Muramatsu, A. Konnoe, K. Okada, *Phys. Chem. Chem. Phys.* 15 (2013) 8088–8094.
- [15] S. Toksabay, S.O. Hacioglu, N.A. Unlu, *Polymer* 55 (2014) 3093–3099.
- [16] A. Bolduc, S. Dufresne, W.G. Skene, *J. Mater. Chem.* 20 (2010) 4820–4826.
- [17] H.M. Wang, S.H. Hsiao, *Polymer* 50 (2009) 1692–1699.
- [18] H.J. Niu, Y.D. Huang, X.D. Bai, X. Li, *Mater. Lett.* 58 (2004) 2979.
- [19] H.J. Niu, Y.D. Huang, X.D. Bai, X. Li, G.L. Zhang, *Mater. Chem. Phys.* 86 (2004) 33.
- [20] X. Zhang, Y.H. Jin, F.S. Du, Z.C. Li, F.M. Li, *Macromolecules* 36 (2003) 3115.
- [21] O. Yoshiyuki, T. Hiroko, *J. Polym. Sci. Pol. Chem.* 28 (1990) 1763–1769.
- [22] S. Kumar, P.K. Dutta, P. Sen, *Carbohydr. Polym.* 80 (2010) 563–569.
- [23] Y.H. Liu, M.H. Liu, *Thin Solid Films* 415 (2002) 248–252.
- [24] J.W. Cai, H.J. Niu, C. Wang, L.N. Ma, X.D. Bai, W. Wang, *Electrochim. Acta* 76 (2012) 229–241.
- [25] C.H. Duan, W.Z. Cai, F. Huang, J. Zhang, M. Wang, T.B. Yang, C.M. Zhong, X. Gong, Y. Cao, *Macromolecules* 43 (2010) 5262–5268.
- [26] K. Zhang, H.J. Niu, C. Wang, X.D. Bai, Y.F. Lian, W. Wang, *J. Electroanal. Chem.* 682 (2012) 101–109.
- [27] S.J. Yoo, J.H. Cho, J.W. Lim, S.H. Park, J. Jang, Y.E. Sung, *Electrochem. Commun.* 12 (2010) 164–167.
- [28] B.H. Peng, G.F. Liu, L. Liu, D.Z. Jia, K.B. Yu, *J. Photochem. Photobiol. A Chem.* 171 (2005) 243–249.
- [29] I. Rousoo, N. Friedman, M. Sheves, M. Ottolenghi, *Biochemistry* 34 (1995) 12059–12065.
- [30] C.J. Drummond, D. Neil, Furlong, *J. Chem. Soc., Faraday Trans.* 86 (1990) 3613–3621.